

KPG 390: A pair of trailing spirals.

P. Repetto¹, M. Rosado¹, R. Gabbasov¹ and I. Fuentes-Carrera²

¹Instituto de Astronomía, Universidad Nacional Autónoma de México (UNAM),
Apdo. Postal 70-264, 04510, México, D.F., México.
email: prepetto@astroscu.unam.mx

²Department of Physics, Escuela Superior de Física y Matemáticas, IPN, U.P. Adolfo López
Mateos, C.P. 07738, Mexico city IPN, México.

Abstract. In this study we present scanning Fabry-Perot H α observations of the isolated interacting galaxy pair NGC 5278/79. We derived velocity fields, various kinematic parameters and rotation curves for both galaxies. These kinematical results together with the fact that dust lanes have been detected in both galaxies, as well as the analysis of surface brightness profiles along the minor axis, allowed us to determine univocally that both components of the interacting pair are trailing spirals. We have also estimated the mass of NGC 5278 fitting its rotation curve with a disk-halo component. We have tested three different types of halo (pseudo-isothermal, Hernquist and Navarro Frenk White) and we have obtained that the rotation curve can be fitted either with a pseudo-isothermal, an Hernquist halo or a Navarro Frenk White halo component, although in the first case the amount of dark matter required is about ten times smaller than for the other two halo distributions.

Keywords. Instrumentation: interferometers, methods: data analysis, techniques: image processing, techniques: interferometric, techniques: radial velocities, astrometry, galaxies: interactions, galaxies: kinematics and dynamics, galaxies: spiral, (cosmology): dark matter.

1. Introduction

Interactions and mergers of galaxies are common phenomena in the Universe. Isolated pairs of galaxies represent a relatively easy way to study interactions between galaxies because these systems, from a kinematical point of view, are simpler than associations and compact groups of galaxies, where so many galaxies participate in the interaction process, that it is difficult to discriminate the role of each galaxy in the interaction.

Obtaining kinematical information on interacting galaxies systems is useful to understand the effect the interacting process could have on each of the members of the pair (Marcelin *et al.* (1987), Amram *et al.* (2002), Fuentes-Carrera *et al.* (2007)). Rotation curves determination, for instance, is a very efficient tool to study the mass distribution in spiral galaxies. It allows to discover the significant discrepancy between the luminous mass and the gravitational mass that has led to the assumption of a large amount of dark matter in the Universe (Rubin *et al.* (1976), Bosma *et al.* (1977), Blais-Ouellette *et al.* (2001)) (among other authors). The decomposition of the rotation curve is made considering various mass components such as bulge, disk and dark matter halo (van Albada *et al.* (1985)).

In this work we study the system NGC5278/79 (Arp 239 KPG 390) belonging to a particular class of interacting pair of galaxies: the M51-type galaxies. According to Reshetnikov & Klimanov(2003), the two empirical criteria to classify an M51-type pair of galaxies are that the B-band luminosity ratio of the components (main/satellite) vary between 1/30 and 1/3, and that the projected distance of the satellite does not exceed two optical diameters of the main component. In the case of NGC5278/79 the B-band

luminosity ratio is 0.30 and the projected separation is 16.8 kpc (optical diameter of the main component is 39.2 kpc).

For this particular system there are HST images (one of these images is showing in Fig. 1) (Windhorst *et al.* (2002)) showing dust lanes across the nuclei of both galaxy components that could help us determine which are the nearest sides of the galaxies and thus, to determine whether the spiral arms are leading or trailing, as well as to have an extensive view of the geometric conditions of the encounter in order to perform numerical simulations. It is important to recall that according to several studies (Byrd *et al.* (1989), Keel (1991)), leading spiral arms can only exist in interacting systems with retrograde encounters triggering the formation of $m = 1$ spiral arms (Athanasoula (1978), Thomasson *et al.* (1989)), conditions that, in principle, taking into account the morphology, could be fulfilled by NGC5278/79.

The aim of this study is to perform detailed kinematic and dynamic analysis of NGC 5278/79 using $H\alpha$ kinematical data in order to study the mass distribution of this pair of galaxies and to determine the type of spiral arms (leading or trailing) in the galaxy members with the intention of reproducing both its morphology and kinematics with future numerical simulations that could shed more light on the interaction process.

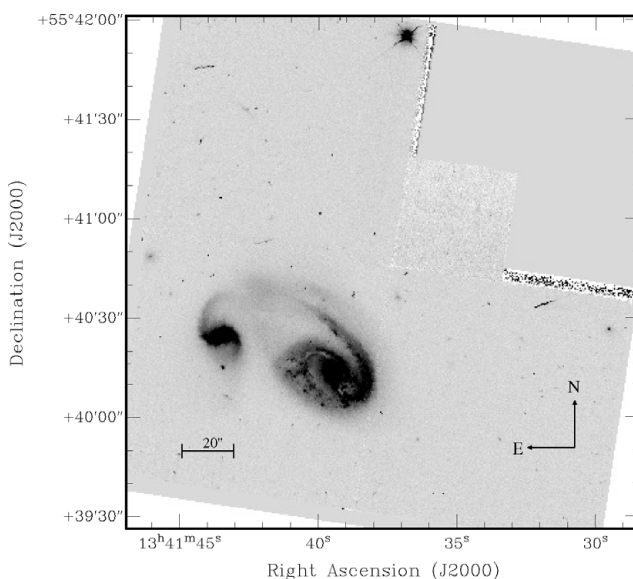


Figure 1. HST image at $\lambda = 8230 \text{ \AA}$ with the F814W filter (Windhorst *et al.* (2002)).

2. Observations and data reduction

Observations of NGC 5278/79 (Arp 239, KPG 390) were done in 2002 July at the $f/7.5$ Cassegrain focus of the 2.1 m telescope at the Observatorio Astronómico Nacional in San Pedro Mártir (México), using the scanning Fabry-Perot interferometer PUMA (Rosado *et al.* (1995)). The data reduction and most of the analysis were done using the ADHOCw† software. For more information about the observations strategy, data reduction and analysis see Repetto *et al.* (2010)

† <http://www.oamp.fr/adhoc/> developed by J. Boulesteix.

3. Velocity field

The total velocity field of KPG 390 with each component of the pair and the bridge, is shown in Fig. 2 with $H\alpha$ isophotes superposed. The outer isophote clearly shows a common envelope enclosing both galaxies.

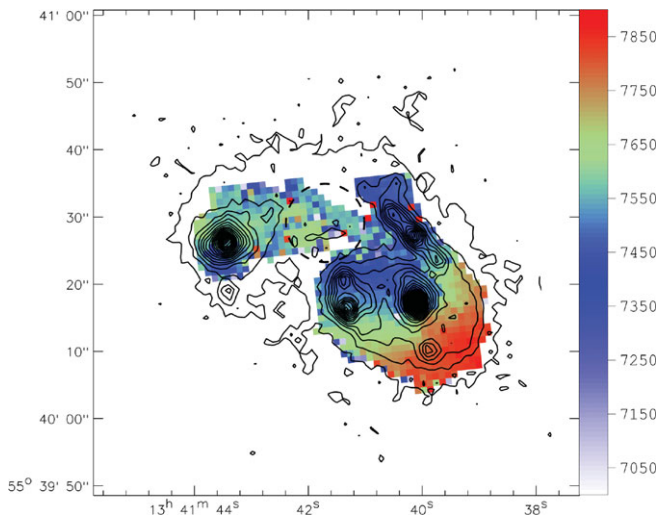


Figure 2. The full velocity field of KPG 390 (Arp 239) with overplotted $H\alpha$ image isophotes. The isophotes are separated by a factor of 200 in arbitrary intensity units and the color scale shows heliocentric systemic velocity in km s^{-1} . The dashed circle indicates the bridge region.

In the disk of NGC 5278 the radial velocity values are in the range $7400 - 7860 \text{ km s}^{-1}$. On the other hand, inside the disk region of NGC 5279 the radial velocity values are in the range ($7550 - 7650 \text{ km s}^{-1}$). For NGC 5279 the mean radial velocity value is of $\approx 7600 \text{ km s}^{-1}$. The radial velocity values in the bright arm region of the primary galaxy (north side of NGC 5278) are in the range $7350 - 7480 \text{ km s}^{-1}$. In this zone the velocity profiles are slightly broader than those in the disk of NGC 5278.

In the bridge region indicated by a dash circle in Fig. 2, the radial velocity profiles are double, or distorted, and the kinematics is more complicated. Such profiles shown in Fig. 3 (region inside the square) have a main radial velocity component and a faint secondary one. In this figure the north part shows profiles with lower signal-to-noise ratio, whereas in the south part the profiles have higher signal to noise ratio. The mean radial velocity of the brightest peak in the double profiles of the bridge region is $\approx 7600 \text{ km s}^{-1}$, which is close to the mean systemic velocity of both galaxies. The faintest velocity component (at $7200 - 7330 \text{ km s}^{-1}$) could be associated with an extended gas outflow due to the interaction.

Summarizing, we conclude that there is a transference of material between the two components of the pair, indicating the ongoing interaction process.

4. Rotation curves

The rotation curves were obtained from the corresponding velocity fields considering that the inner parts of these two galaxies are not strongly perturbed by the interaction process. This is true at least up to a certain radius. In the case of NGC 5278 this radius is $\approx 7 \text{ kpc}$ ($\approx 14''$) and for NGC 5279 it is $\approx 6 \text{ kpc}$ ($\approx 12''$). Thus, we can accurately

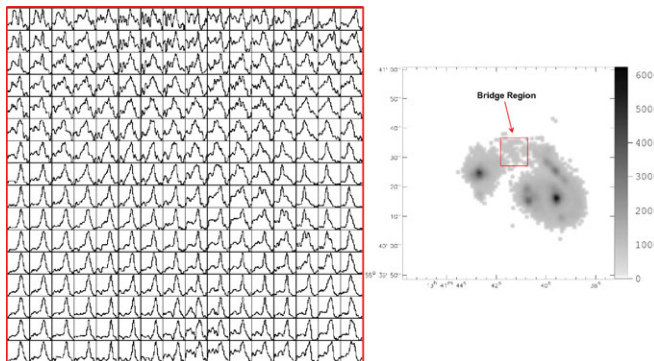


Figure 3. H α radial velocity profiles showing the region of interaction between the two galaxies, superposed onto the H α image of KPG 390. The profiles are normalized by the corresponding intensity in each pixel. The square indicates the region of double profiles displayed on the left. These are the original spectra.

determine the rotation curve of both galaxies considering a region of the velocity field within a sector of a specified angle inside these radii.

4.1. NGC 5278

The rotation curve of NGC 5278 was obtained with pixels in the velocity field within an angular sector of 20° around the galaxy major axis. The photometric center of this galaxy is the position of the brightest pixel in the continuum map. The physical coordinates of the photometric center are R.A. = 13^h 41^m 39.36^s and Dec. = 55° 40' 47.13". The kinematic center, derived as the position around the photometric center at which the scatter in rotation curve is minimized, is R.A. = 13^h 41^m 39.33^s and Dec. = 55° 40' 44.39".

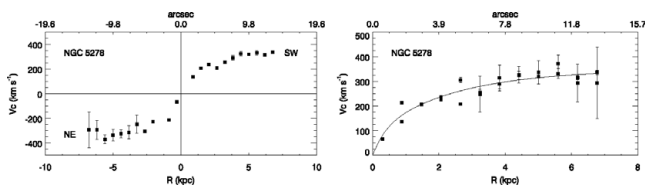


Figure 4. *Left:* Rotation curve of NGC 5278 for both sectors of the galaxy superposed: approaching (NE) and receding (SW) part. *Right:* Overplotted both parts of the rotation curve together with an exponential fit. The error bars are dispersion of values within the considered sector.

The kinematic parameters that give us the most symmetric, smooth, and low-scattered curve inside a radius of 12" are P.A. = (42 ± 2)°, *i* = (42 ± 2)°, and $V_{sys} = (7627 \pm 10)$ km s⁻¹. The corresponding rotation curve is shown in Fig. 4.

4.2. NGC 5279

The brightest pixel of NGC 5279 in our continuum map has coordinates: R.A. = 13^h 41^m 44.240^s and Dec. = 55° 41' 1.45". The coordinates of the kinematical center are R.A. = 13^h 41^m 43.901^s and Dec. = 55° 41' 0.32".

The kinematic parameters that reduce significantly the asymmetry and scatter in the rotation curve were in this case: P.A. = (141.5 ± 1)°, *i* = (39.6 ± 1)° and $V_{sys} = (7570 \pm 10)$ km s⁻¹. Due to the lack of data points it was impossible to minimize the scattering and asymmetries of the rotation curve. The asymmetry of the rotation curve did not allowed

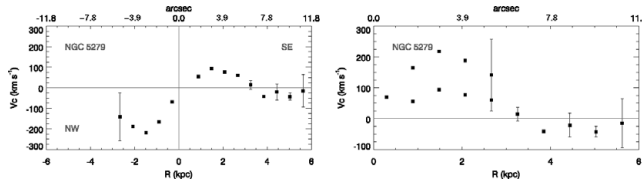


Figure 5. *Left:* Rotation curve of NGC 5279 for both sectors of the galaxy: approaching (NW) and receding (SE) side. *Right:* Overplotted both parts of the rotation curve. The error bars represent dispersion of velocity points within the considered sector.

us to perform a detailed analysis of the mass distribution of NGC 5279. The corresponding rotation curve is shown in Fig. 5.

5. Rotation curve decomposition of NGC 5278

We consider that NGC 5278 has two components that contribute to the rotation curve: an exponential disk and a massive dark matter (DM) halo. The disk was assumed to be thin and not truncated with an exponential density distribution (Freeman (1970)).

Photometric observations provide the surface brightness profiles from which we can obtain the central surface brightness in magnitude units and the disk scale length in kpc. In order to transform these observable parameters to mass density distribution, it is assumed that the M/L ratio is uniform and constant over the disk. In principle, the disk M/L could be known from photometric and spectroscopic observations of the disk which allow us to know the colors, or to perform a population synthesis analysis. In this case we do not have any detailed photometric study of KPG 390 so, we perform the rotation curve decomposition for NGC 5278 using the photometric data given by Mazzarella & Boroson (1993) and Paturel *et al.* (2003) as upper limits.

We tested three different types of DM halos: Hernquist halo Hernquist (1990), Navarro, Frenk & White halo (NFW) Navarro *et al.* (1996), and spherical pseudo-isothermal halo. To accomplish the rotation curve decomposition we fit the rough rotation curve data using an exponential function (Fig. 4). Then we use this fit to perform the disk-halo decomposition.

Since for this galaxy we do not have any robust restriction on the luminous mass distribution, we vary the disk scale radius $h \in [1.0 - 11.0]$ kpc and the mass to luminosity ratio $M/L_B \in [1.3 - 6.3]$. The halo mass and the halo scale length are in the range $[0 - 10^{13}] M_\odot$ and $[0 - 20]$ kpc.

The rotation curve of NGC 5278 can be well fitted with spherical pseudo-isothermal halo, Hernquist halo and NFW halo (Fig. 6). The results obtained are summarized in Table 1.

6. NGC 5278/79: two trailing spirals

This kinematic study sheds light on the geometry of the galaxy encounter by determining the real orientation in the sky of the galaxy members, as well as the kind of spiral arms they possess. The latter point is not irrelevant in the case of interacting systems where a possibility of having leading spiral arms is open. Indeed, even if leading spiral arms in galaxies are a very uncommon phenomenon, the only examples where are found are interacting systems.

Following Sharp & Keel(1985) there is a criterion that determines if any particular spiral galaxy has trailing or leading arms. This criterion is based on three main clues

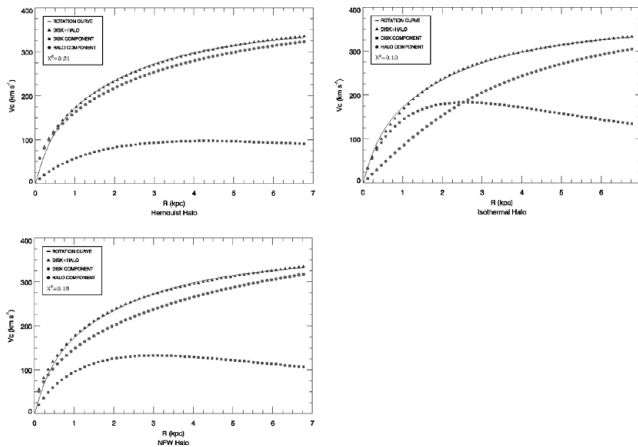


Figure 6. Disk-Halo decomposition of the rotation curve of NGC 5278.

Table 1. Mass determination from rotation curve decomposition.

Rotation curve mass	Pseudo-isothermal ^a	Hernquist	NFW
Disk component (M_{\odot})	2.42×10^{10}	1.13×10^{10}	1.5×10^{10}
Disk length scale (kpc)	1.2	2.0	1.42
Disk M/L	2.8	1.3	1.6
Halo component (M_{\odot})	1.9×10^{11}	2.1×10^{12}	6.3×10^{12}
Halo length scale (kpc)	2.8	17.7	16.8
Total Mass (M_{\odot})	2.1×10^{11}	2.1×10^{12}	6.3×10^{12}
χ^2 ^b	0.10	0.21	0.18

^a Maximum Disk

^b Normalized χ^2 by 58 degrees of freedom.

(receding-approaching side, direction of spiral arms and the tilt of the galaxy, i.e., which side is closer to observer).

In our particular case, we have both the kinematic information in order to establish which side of the galaxy is receding and which side approaching, as well as very conspicuous morphological aspects such as well defined spiral arm patterns and the presence of dust lanes in both galaxy members running near the galaxy nuclei. This last issue will be used in what follows in two main ways: 1) we will suspect that the nearest side of the galaxy is the side hosting the dust lane and, 2) we will check it by getting an intensity profile of the galactic nucleus along the minor axis. In this kind of profiles, the nearest side is the steepest one (because of the presence of the dust lane).

In the case of NGC 5278, the receding radial velocities are in the south-western part, while the approaching radial velocities are at the north-eastern side. From Fig. 1 it is clear that the arms of NGC 5278 point in anti-clockwise direction and the dust lane is located at the concave side of the bulge, thus the northern side is the nearest. This fact is confirmed by the profile extracted along the kinematic minor axis of NGC 5278 (see Fig. 7). From these figures and the above criteria we have decided that NGC 5278 is a trailing spiral because the sense of rotation is opposite to the direction of the arms. We were able to apply similar arguments to NGC 5279. In this case the receding radial velocities are at the north-eastern side of the galaxy and the approaching radial velocities are at the south-western part. The arms of NGC 5279 point in clockwise direction and the nearest side is the southern side. As in the case of NGC 5278 this fact is confirmed by the profile extracted along the kinematic minor axis of NGC 5279 (see Fig. 7) Väisänen

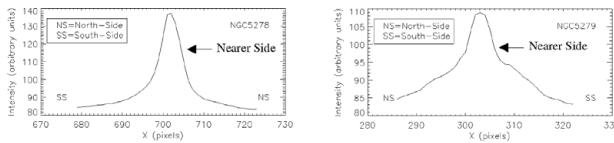


Figure 7. Intensity profiles along the kinematic minor axis of NGC 5278 and NGC 5279. The cross-section is captured in the Hubble image (Fig. 1). From the profile on left it is clear that the northern-side is the nearer in NGC 5278, because the profiles fall more abruptly than along the southern-side. In the case of NGC 5279 the southern-side is the nearer because the profiles fall more abruptly than along the northern-side, as one can see from the profile on right.

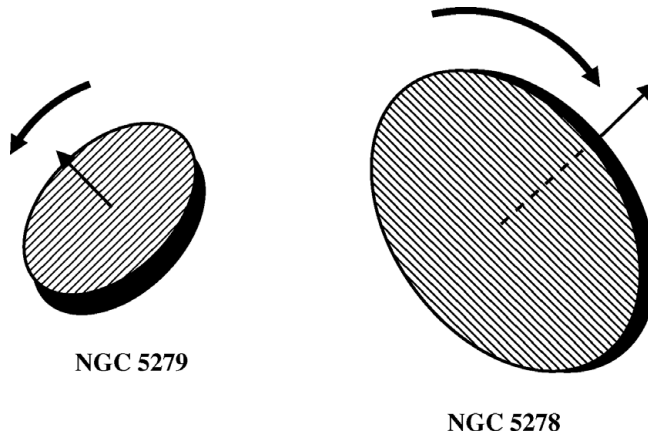


Figure 8. A possible spatial configuration of KPG 390.

et al. (2008). We can conclude that NGC 5279 is a trailing spiral also because the sense of rotation is opposite to the direction of the arms. A scheme of 3D orientation of KPG 390 derived from our kinematic analysis is shown in Fig. 8.

7. Conclusions

In this work we presented Fabry-Perot observations of the isolated pair of galaxies NGC 5278/79 (Arp 239, KPG 390) showing that for an interacting and asymmetric system it is important to have kinematic information of large portions of the galaxies participating in the interaction process. From the analysis of the velocity field, we obtain the rotation curves for NGC 5278 and NGC 5279. We perform the decomposition of the rotation curve for NGC 5278 and determine the content of dark matter of this galaxy, using different types of halos (pseudo-isothermal, Hernquist and NFW halo). We also study the kind of spiral arms of the two spirals of the pair and we determine that NGC 5278/79 are trailing spirals. We will use the kinematic information as a starting point in future numerical simulations of this pair.

Acknowledgements

We acknowledge DGAPA-UNAM grant: IN102309 and CONACYT grant: 40095-F.

References

- Marcelin, M., Lecoarer, E., Boulesteix, J., Georgelin, Y., & Monnet, G. 1987, *A&A*, 179, 101
- Amram, P., Mendes de Oliveira, C., Plana, H., Balkowski, C., Boulesteix, J. & Carignan, C. 2002, *Ap&SS*, 281, 389
- Fuentes-Carrera, I., Rosado, M., Amram, P., Salo, H. & Laurikainen, E. 2007, *A&A*, 466, 847
- Rubin, V. C., Peterson, C. J. & Ford, W. K., Jr. 1976, *BAAS*, 8, 297
- Bosma, A., van der Hulst, J. M. & Sullivan, W. T., III 1977, *A&A*, 57, 373
- Blais-Ouellette, S., Amram, P. & Carignan, C. 2001, *AJ*, 121, 1952
- van Albada, T. S., Bahcall, J. N., Begeman, K. & Sancisi, R. 1985, *ApJ*, 295, 305
- Reshetnikov, V. P. & Klimanov, S. A. 2003, *Astron. Lett.*, 29, 429
- Windhorst, R. A., *et al.* 2002, *ApJS*, 143, 113
- Byrd, G. G., Thomasson, M., Donner, K. J., Sundelius, B., Huang, T. Y. & Valtonen, M. J. 1989, *Celestial Mechanics*, 45, 31
- Keel, W. C. 1991, *ApJ*, 375, L5
- Athanassoula, E. 1978, *A&A*, 69, 395
- Thomasson, M., Donner, K. J., Sundelius, B., Byrd, G. G., Huang, T.-Y. & Valtonen, M. J. 1989, *A&A*, 211, 25
- Freeman, K. C. 1970, *ApJ*, 160, 811
- Hernquist, L. 1990, *ApJ*, 356, 359
- Navarro, J. F., Frenk, C. S. & White, S. D. M. 1996, *ApJ*, 462, 563
- Sharp, N. A. & Keel, W. C. 1985, *AJ*, 90, 469
- Väisänen, P., Ryder, S., Mattila, S. & Kotilainen, J. 2008, *ApJ*, 689, L37
- Mazzarella, J. M. & Boroson, T. A. 1993, *ApJS*, 85, 27
- Paturel, G., Petit, C., Prugniel, P., Theureau, G., Rousseau, J., Brouty, M., Dubois, P., & Cambrésy, L. 2003, *A&A*, 412, 45
- Rosado, M., *et al.* 1995, *Rev. Mexicana AyA*, 3, 263
- Repetto, P., Rosado, M., Gabbasov, R. & Fuentes-Carrera, I. 2010, *AJ*, 139, 1600

Discussion

WOLF: Why is there a factor of 3 discrepancy between total halo mass when adopting a NFW vs Hernquist profile? Also, how do you define the total halo mass for the NFW? What is your cutoff radius?

REPETTO: This discrepancy is due to the fact that we chose the solution with the minimum χ_2 value; however, there were other solutions with higher χ_2 but similar halo masses. The total halo mass for the NFW halo was defined following Navarro *et al.* (1996) as M_{200} and the cutoff radius was defined as R_{200} . In the case of NGC 5278 the cutoff radius was located at ≈ 234 kpc.